2004

Connexin expression and conducted vasodilation along arteriolar endothelium in mouse skeletal muscle

Robin Looft-Wilson

G. W. Payne

S. S. Segal

J Appl Physiol 97: 1152–1158, 2004.
First published May 28, 2004; 10.1152/japplphysiol.00133.2004.

HIGHLIGHTED TOPIC | *Skeletal and Cardiac Muscle Blood Flow*

Connexin expression and conducted vasodilation along arteriolar endothelium in mouse skeletal muscle

Robin C. Looft-Wilson,* Geoffrey W. Payne,* and Steven S. Segal

The John B. Pierce Laboratory, New Haven 06519; and Department of Cellular and Molecular Physiology, Yale University School of Medicine, New Haven, Connecticut 06520

Submitted 4 February 2004; accepted in final form 25 May 2004

Looft-Wilson, Robin C., Geoffrey W. Payne, and Steven S. Segal. Connexin expression and conducted vasodilation along arteriolar endothelium in mouse skeletal muscle. *J Appl Physiol* 97: 1152–1158, 2004. First published May 28, 2004; 10.1152/japplphysiol.00133.2004.—Functional hyperemia requires the coordination of smooth muscle cell relaxation along and between branches of the arteriolar network. Vasodilation is conducted from cell to cell along the arteriolar wall through gap junction channels composed of connexin protein subunits. Within skeletal muscle, it is unclear whether arteriolar endothelium, smooth muscle, or both cell layers provide the cellular pathway for conduction. Furthermore, the constitutive profile of connexin expression within the microcirculation is unknown. We tested the hypothesis that conducted vasodilation and connexin expression are intrinsic to the endothelium of arterioles (17 ± 1 μm diameter) that supply the skeletal muscle fibers in the cremaster of anesthetized C57BL/6 mice. ACh delivered to an arteriole (500 ms, 1-μA pulse; 1-μm micropipette) produced local dilation of 17 ± 1 μm; conducted vasodilation observed 1 mm upstream was 9 ± 1 μm ($n = 5$). After light-dye treatment to selectively disrupt endothelium (250-μm segment centered 500 μm upstream, confirmed by loss of local response to ACh while constriction to phenylephrine and dilation to sodium nitroprusside remained intact), we found that conducted vasodilation was nearly abolished (2 ± 1 μm; $P < 0.05$). Whole-mount immunohistochemistry for connexins revealed punctate labeling at borders of arteriolar endothelial cells, with connexin40 and connexin37 in all branches and connexin43 only in the largest branches. Immunoreactivity for connexins was not apparent in smooth muscle or in capillary or venular endothelium, despite robust immunolabeling for α-actin and platelet endothelial cell adhesion molecule-1, respectively. We conclude that vasodilation is conducted along the endothelium of mouse skeletal muscle arterioles and that connexin40 and connexin37 are the primary connexins forming gap junction channels between arteriolar endothelial cells.

microcirculation; muscle blood flow; gap junctions

MUSCLE BLOOD FLOW IS CONTROLLED through changes in vascular resistance. Within the muscle, arteriolar networks govern the distribution and magnitude of regional blood flow to muscle fibers. In response to muscle contraction, vasodilation originating in distal arterioles can "ascend" into proximal arterioles and their feeding arteries, thereby increasing total blood flow into the muscle (14, 28). This coordinated behavior of resistance networks is attributable to the conduction of vasoactive signals (e.g., hyperpolarization) from cell to cell through gap junction channels along the vessel wall (11, 23, 33, 36).

A key physiological determinant of conducted vasodilation is which layer of the arteriolar wall, endothelium or smooth muscle, provides the cellular pathway for cell-to-cell signal transmission (2, 23, 33). The gap junction channels that couple adjacent cells are composed of connexin proteins, and at least three connexin isoforms (Cx) have been identified in the vasculature: Cx37, Cx40, and Cx43 (8, 17, 25). Connexin-knockout mice have provided some insight into the role of respective connexin molecules in the conduction of vasomotor responses (7, 13). However, little is known of the constitutive expression profile for connexins in arterioles of the mouse. Furthermore, because respective connexin isoforms differ in their biophysical properties and mechanisms of regulation (8, 24), identifying which connexins are expressed in respective branches and cell types may provide new insight into regional differences in vasomotor control (1, 14, 31).

The present experiments used the thin, flat cremaster preparation to study the intact microcirculation of mouse skeletal muscle (7, 13, 18). Using light-dye treatment (LDT) to selectively damage cells of the arteriolar wall in vivo (2), we tested the hypotheses that conducted vasodilation requires an intact endothelium. In complementary experiments, immunohistochemistry was performed on whole-mount muscles to define the distribution and cellular localization of Cx37, Cx40, and Cx43.

MATERIALS AND METHODS

Animal Care and Surgery

All procedures were approved by the Institutional Animal Care and Use Committee of the John B. Pierce Laboratory and were performed in accordance with the Institute for Laboratory Animal Research *Guide for the Care and Use of Laboratory Animals*. Male C57BL/6 mice (~30 g and 9 wk old, $n = 29$) were housed at ~24°C on a 12:12-h light-dark cycle with free access to food and water. Each mouse was anesthetized with pentobarbital sodium (50 mg/kg ip), which was supplemented as needed to prevent withdrawal from toe pinch. At the end of an experiment or after muscle tissue was obtained, the mouse was euthanized with an intraperitoneal overdose injection of pentobarbital sodium.

The anesthetized mouse was placed supine on a transparent acrylic platform. The left cremaster muscle was prepared as described (18).

* R. C. Looft-Wilson and G. W. Payne contributed equally to this work.

Address for reprint requests and other correspondence: S. S. Segal, The John B. Pierce Laboratory, Yale Univ. School of Medicine, 290 Congress Ave., New Haven, CT 06519 (E-mail: sssegal@jbpierce.org).

The costs of publication of this article were defrayed in part by the payment of page charges. The article must therefore be hereby marked "*advertisement*" in accordance with 18 U.S.C. Section 1734 solely to indicate this fact.

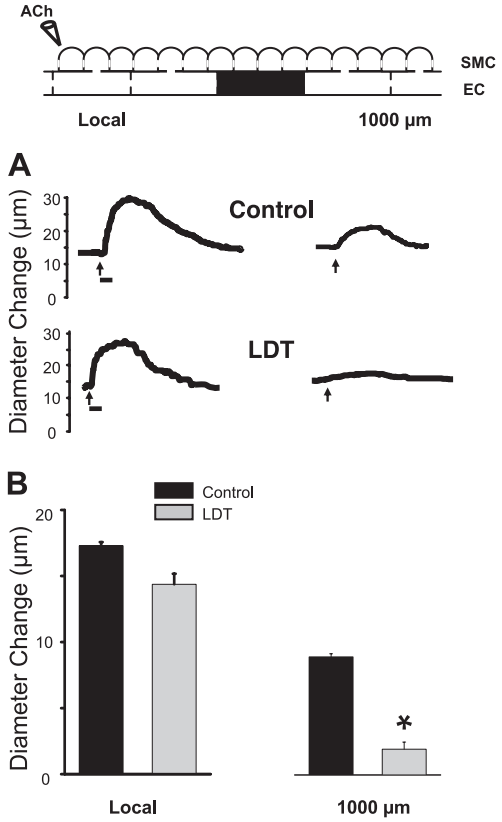

Fig. 1. Disruption of conducted vasodilation with light-dye treatment (LDT; darkened region in *inset* above *A*) of arteriolar endothelium. *Top*: longitudinal section through one edge of vessel wall (not to scale), indicating sites along arteriole where diameter was observed (local vasodilation was at stimulus site, conducted vasodilation was 1,000 μm upstream). SMC, smooth muscle cells; EC, endothelial cells. *A*: representative traces illustrating that LDT had no effect on local vasodilation to ACh (*left* traces) but inhibited conducted vasodilation (*right* traces). Arrows in each trace indicate delivery of ACh stimulus at local site; scale bar, 5 s. *B*: summary data for local and conducted vasodilation following LDT (mean ± SE; $n = 5$). *Significant difference in response to ACh (i.e., loss of conducted vasodilation) before and after LDT observed 1,000 μm from local site of stimulation, $P < 0.05$.

Briefly, a midline incision was made along the ventral surface of the left scrotal sac, and the exposed cremaster muscle was opened longitudinally and separated from the testis, which was repositioned in the abdominal cavity. The muscle was spread radially and pinned onto a pedestal of transparent Sylgard (Dow Corning, Midland, MI) while superfused continuously (5 ml/min) with a bicarbonate-buffered physiological salt solution (PSS; 34°C, pH 7.4) of the following composition (in mM): 137 NaCl, 4.7 KCl, 1.2 $MgSO_4$, 2 $CaCl_2$, and 18 $NaHCO_3$. The PSS was equilibrated with 5% CO_2-95% N_2 unless noted. Chemicals and reagents were purchased from Sigma-Aldrich (St. Louis, MO) and J. T. Baker (Phillipsburg, NJ), unless otherwise indicated.

Intravital Microscopy

The preparation was transferred to the stage of a microscope (modified model 20T, Zeiss), equilibrated for at least 60 min, and viewed with brightfield illumination [Zeiss ACH/APL condenser, numerical aperture (NA) = 0.32]. Esophageal temperature was maintained at 37–38°C with radiant heat. A second-order arteriole was located in the central region of the tissue, which we observed using a Zeiss UD40 objective (NA = 0.41) coupled to a video camera (Hamamatsu model C2400); total magnification on the video monitor (Sony model PVM-132) was ×950. We determined vessel diameter from the edges of the lumen using a video caliper with spatial resolution of ≤1 μm. We acquired data at 40 Hz using a PowerLab system (model 8S, ADI Instruments, Castle Hill, Australia) coupled to a personal computer.

One arteriole was studied in each mouse. Only vessels that exhibited spontaneous vasomotor tone and constricted during 10-min exposure to elevated oxygen (21% with 5% CO_2-74% N_2) were examined. To measure conducted responses, ACh was applied to a discrete site on the downstream end of the arteriole with microiontophoresis (18). A micropipette (internal tip diameter of 1–2 μm) was positioned with its tip adjacent to the arteriole, and a brief pulse (500 ms, 1 μA) of ACh was delivered. Retain current was ≤200 nA. The local change in internal diameter was recorded at the site of ACh delivery, and conducted vasodilation was evaluated at 1,000 μm upstream.

Light-Dye Treatment

The carotid artery was cannulated with PE-10 tubing for injection of FITC conjugated to dextran (70 kDa, 1.0% solution, 1 ml/kg; Sigma Chemical) to retain the fluorochrome within the vascular compartment (2, 4). Midway between the original "local" site of ACh delivery and the upstream site for evaluating conducted vasodilation, a segment (~250 μm long) of the arteriole was illuminated (excitation of 450–490 nm, emission of >520 nm; Zeiss filter 487709) through an immersion objective (×40, NA = 0.75; Zeiss) with a 75-W Xenon lamp. Illumination was continued until vasodilation was observed to begin (4–6 min), indicating disruption of the endothelium. The arteriole then recovered for ~5 min. In arterioles of the hamster cheek pouch, if illumination continues beyond this point, damage proceeds into the smooth muscle layer and vasoconstriction occurs (2). To

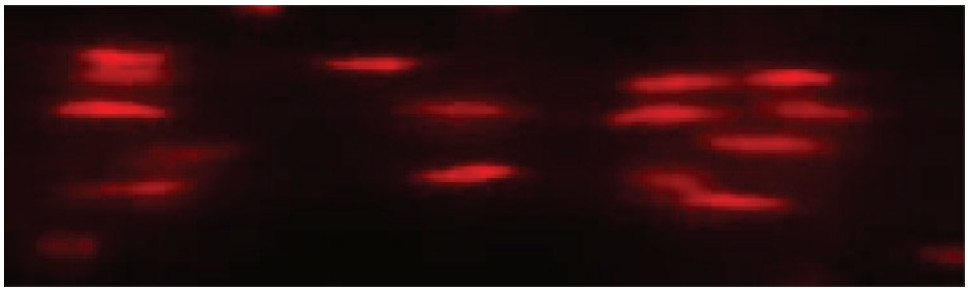

Fig. 2. Dye labeling of endothelial cell nuclei after prolonged LDT. Duration of illumination was extended until vasoconstriction was observed (~20 min). Propidium iodide was then perfused through the vessel lumen (see MATERIALS AND METHODS for details). This nuclear dye is excluded from healthy cells and taken up by those cells in which the permeability barrier of the plasma membrane has been compromised. Illumination for the duration required to disrupt conduction (4–6 min) did not produce dye labeling. Endothelial cell nuclei orient along the axis of the arteriole. Image was acquired with ×20 objective (field width = 125 μm, height = 40 μm).

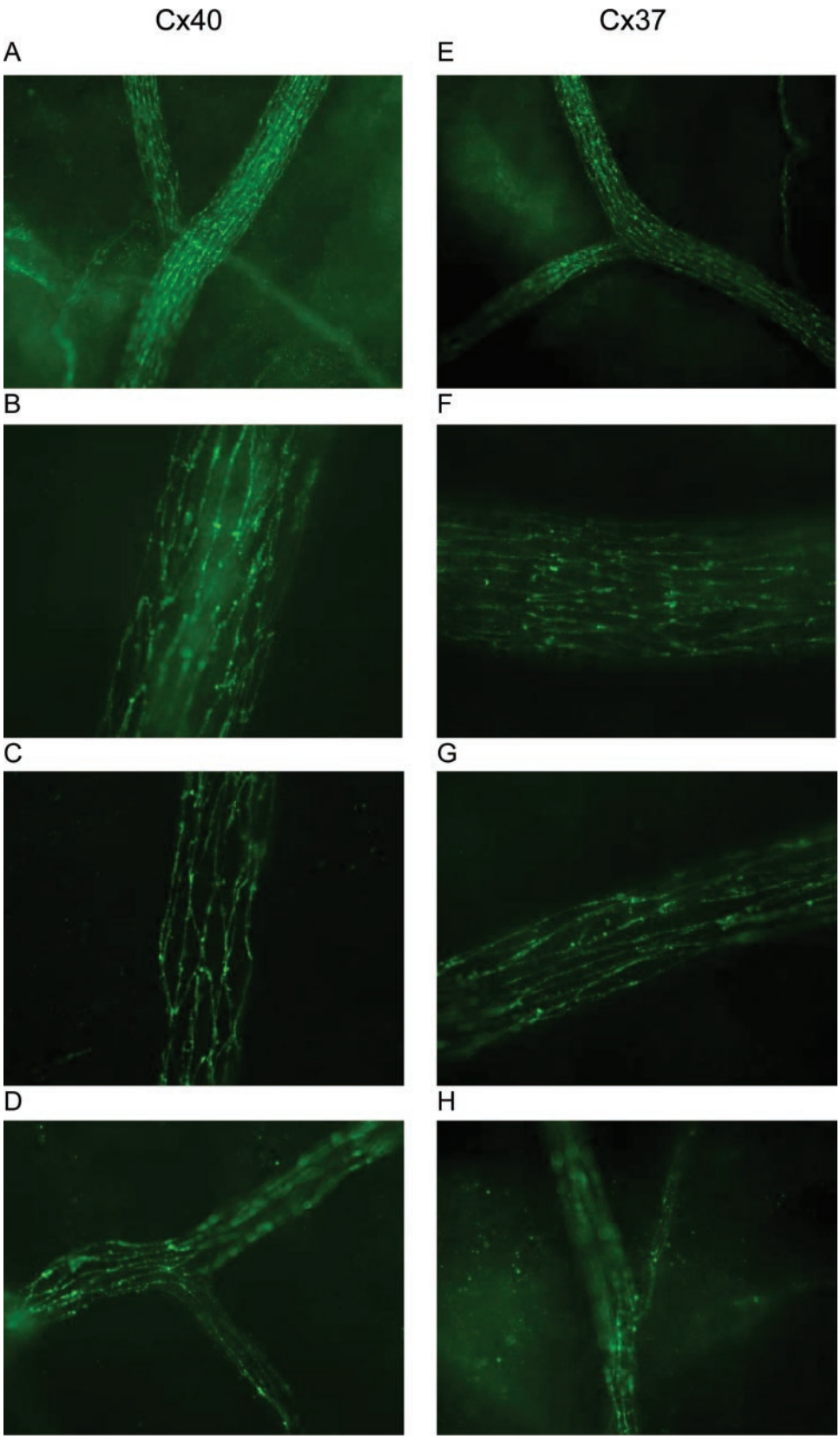

Fig. 3. Expression of connexin isoforms Cx37 and Cx40 in mouse cremaster muscle. *A–D*: Cx40. *E–H*: Cx37. *A* and *E*: images of large arterioles acquired with ×20 objective (field width = 445 μm, height = 350 μm). *B* and *F*: images of large arterioles acquired with ×60 objective (field width = 145 μm, height = 115 μm). *C*, *D*, *G*, *H*: images of intermediate arterioles acquired with ×60 objective. Note consistent punctate labeling around endothelial cell borders. See *Whole-Mount Immunohistochemistry* in MATERIALS AND METHODS for explanation of "large" and "intermediate."

evaluate such an effect here, additional experiments ($n = 3$) were performed in which LDT was continued until vasoconstriction occurred in the region of illumination. At this time, the aorta was cannulated and the vasculature was perfused with propidium iodide (1 μM in PSS; Molecular Probes, Eugene, OR). Although propidium iodide is excluded from healthy cells, it becomes permeant after disruption of membrane integrity (2).

To evaluate the effect of LDT on endothelial cell integrity, the ACh micropipette was repositioned at the site of illumination, where the loss of local responses to ACh delivery confirmed disruption of the endothelium (2, 4). We evaluated smooth muscle cell integrity at the site of LDT using microiontophoresis of phenylephrine (0.5 M, 500 ms). The ACh micropipette was repositioned at the original downstream site, and the ability of vasodilation to conduct through the site of LDT was reevaluated 1,000 μm upstream. Maximal diameter was then recorded at the site of LDT during topical application of 10 μM sodium nitroprusside (SNP). Time controls verified that local and conducted responses to ACh remained stable for the duration of these experiments (2–3 h).

Whole-Mount Immunohistochemistry

For immunolabeling experiments, cremaster muscles were dissected bilaterally (as above) from each mouse and superfused with PSS containing SNP. Using a stereomicroscope (magnification of ×7–40), we drew detailed maps of principal arteriolar and venular networks to identify respective vessel branches during subsequent analysis. Vessel branch orders were generally classified according to diameter: "large" refers to arterioles and venules >30 μm, and "intermediate" refers arterioles and venules 12–30 μm (26). A muscle was then severed from its origin and fixed with 4% formaldehyde in PBS for 10 min, washed with PBS (1.0 mM NaH_2PO_4, 8.1 mM Na_2HPO_4, and 154 mM NaCl, pH 7.4) (2 × 15 min), blocked, and permeabilized for 1 h in 2% BSA-0.2% Triton X-100-PBS. It was then incubated in 0.05% Chicago Sky Blue in PBS for 5 min (to reduce background fluorescence), washed 3 × 10 min in PBS, and incubated in primary antibody [all from rabbit; Cx43 at 1:200 (Sigma Chemical), Cx40 at 1:400 (Chemicon International, Temecula, CA), and Cx37 at 1:400 (Alpha Diagnostic International, San Antonio, TX)] overnight at 4°C. Each preparation was labeled for one connexin isoform. Tissues were washed 2 × 30 min in 1% Triton X-100-PBS and for 30 min in PBS and then incubated in secondary antibody (goat anti-rabbit Alexa-488, Molecular Probes, diluted 1:800) for 1 h at room temperature.

Controls were performed with identical procedures to confirm the integrity and accessibility of antibodies to endothelium and smooth muscle of microvessels embedded in the cremaster muscle. For endothelial cells, cremaster muscles were incubated with platelet endothelial cell adhesion molecule (PECAM)-1 antibody (from rabbit, 1:500; a generous gift from J. Madri) followed by goat anti-rabbit Alexa-488. For smooth muscle cells, cremaster muscles were incubated with smooth muscle α-actin antibody (Dakocytomation, Capenteria, CA; mouse MAb, 1:200), followed by goat anti-mouse Alexa-488 (1:800). To confirm the lack of nonspecific labeling for secondary antibodies, additional muscles were treated identically as connexin-labeled muscles, except for the omission of primary antibody.

After exposure to the secondary antibody, specimens were washed 2 × 30 min in 1% Triton X-100-PBS and 30 min in PBS and mounted on a slide with Vectashield (Vector Laboratories, Burlingame, CA). We examined each preparation visually in detail at different magnifications by following microvascular networks and focusing through the tissue. We used a fluorescence microscope (E800, Nikon, Melville, NY; ×20/0.50 plan fluor and ×60/1.40 oil objectives) to obtain representative images, which were prepared using Adobe Photoshop (Adobe Systems, San Jose, CA). The pattern of labeling clearly identified whether the endothelium (axial orientation) or the smooth muscle (circumferential orientation) cell type expressed immunoreactive protein (25). Specificity of primary antibodies for connexins was verified with the use of cultured cells expressing specific connexin isoforms (25).

Data Analysis

Vasomotor responses to ACh, phenylephrine, and SNP were calculated as follows: diameter change = (peak response diameter − resting diameter) at respective sites of observation. Data were analyzed with one-way repeated-measures ANOVA with Tukey's post hoc comparisons (Sigma Stat 2.03; SPSS, Chicago, IL). Differences between groups were accepted as statistically significant at $P < 0.05$. Summary data are presented as means ± SE. Values of n for intravital microscopy refer to the number of arterioles studied in vivo from as many mice. For immunohistochemistry, n refers to the number of whole-mount muscle preparations analyzed with the designated antibody. For a given antibody, each muscle was taken from a different mouse.

RESULTS

Conduction of Vasodilation Along Arteriolar Endothelium

Arterioles studied for conduction had an in vivo resting diameter of 17 ± 1 μm ($n = 5$) and constricted reversibly by ~5–10 μm during the 10-min equilibration with 21% oxygen. Local vasodilation to ACh under control conditions was consistently >15 μm (Fig. 1). With ACh delivered at the site of LDT, local dilation was 1 ± 1 μm, confirming endothelial cell disruption. The conducted response increased the diameter by ~50% under control conditions and was nearly abolished after LDT (Fig. 1). Conduction was eliminated in two experiments

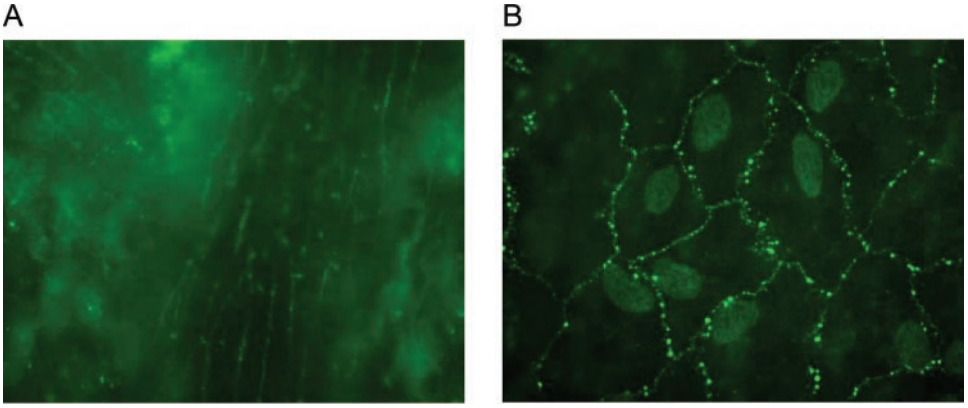

Fig. 4. Expression of Cx43 in mouse cremaster muscle. *A*: large arteriole. Note diffuse autofluorescence of adventitia surrounding punctate labeling of endothelial cell borders (arteriole is oriented vertically in middle of field). *B*: mesothelial cell layer. Note punctate labeling around mesothelial cell borders and diffuse labeling throughout nuclei. See *Whole-Mount Immunohistochemistry* in MATERIALS AND METHODS for explanation of "large." Images were acquired with ×60 objective (field width = 145 μm, height = 115 μm).

and attenuated by >70% in three experiments. These residual conducted responses may be attributed to incomplete disruption of the endothelium as a conduction pathway (4), as care was taken to minimize damage to surrounding smooth muscle cells. We confirmed integrity of smooth muscle cell function after selective disruption of the endothelium by the preservation of basal tone at the site of LDT (17 ± 2 μm resting diameter) while vasoconstriction to phenylephrine (control: 10 ± 1 μm, post-LDT: 9 ± 1 μm) and dilation to SNP (15 ± 1 μm) remained intact. With illumination continued until endothelial cells labeled with propidium iodide (Fig. 2, $n = 3$), smooth muscle cells contracted and no longer responded to phenylephrine.

Connexin Protein Expression

Endothelium. Labeling for Cx37 ($n = 10$) and for Cx40 ($n = 9$) was apparent in endothelial cells of all branch orders of arterioles (Fig. 3) in each respective tissue. In contrast, relatively weak labeling for Cx43 ($n = 9$) was present in the endothelium of large arterioles (Fig. 4) in six of nine preparations but not in the smaller branches. Remarkably, Cx43 labeled clearly at the borders of mesothelial cells (which line the ventral surface of the cremaster muscle) in all nine of these tissues (Fig. 4), confirming the consistency and efficacy of the Cx43 antibody in the mouse cremaster muscle. Immunoreactivity was not apparent in capillary or venular endothelium for Cx37, Cx40, or Cx43. Nevertheless, robust labeling for PECAM-1 in arterioles, capillaries, and venules verified that antibodies had similar access to all microvessels (Fig. 5*A*).

Smooth muscle. There was no evidence of connexin immunoreactivity in either arteriolar or venular smooth muscle. However, immunolabeling with smooth muscle α-actin confirmed that smooth muscle cells were intact and accessible to antibodies (Fig. 5*B*; $n = 3$). Background fluorescence was negligible in the absence of primary antibodies (Fig. 5*C*).

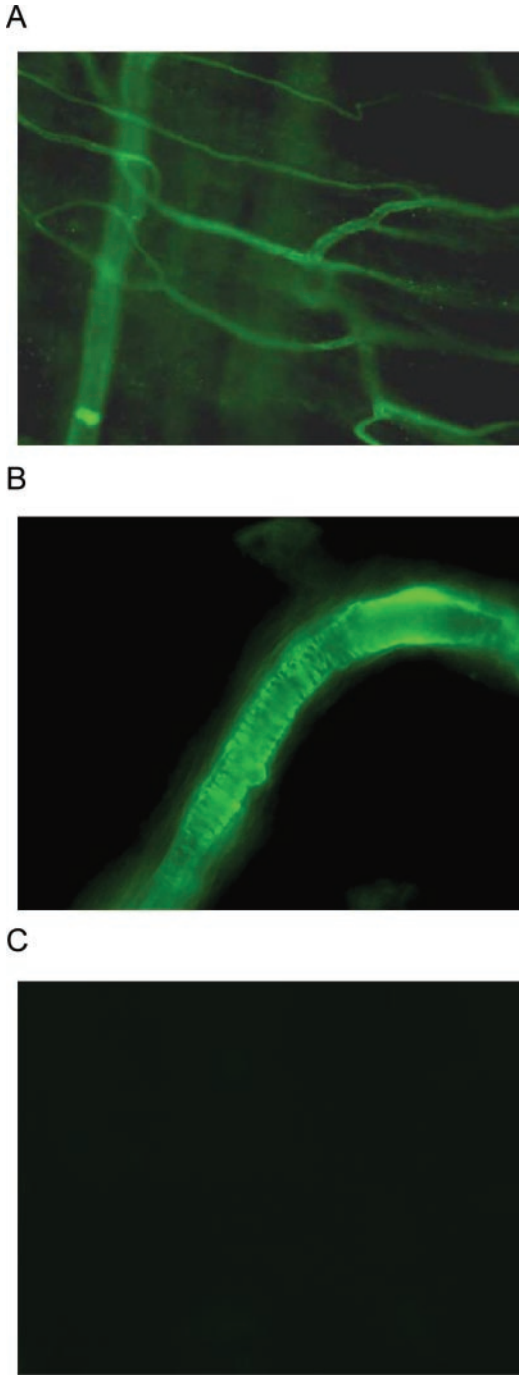

Fig. 5. Control experiments for whole-mount immunohistochemistry in mouse cremaster muscle. *A*: platelet endothelial cell adhesion molecule-1 labeling in microvascular network. *B*: smooth muscle α-actin labeling smooth muscle cells in an arteriole curving in and out of focal plane. *C*: negligible labeling in the absence of a primary antibody. Images were acquired with ×60 objective (field width = 145 μm, height = 115 μm).

DISCUSSION

Muscle blood flow increases with the metabolic demand of active muscle fibers. Although the role of vasodilator metabolites in promoting functional hyperemia has long been a focus of research efforts, much less is known about how the relaxation of smooth muscle cells is coordinated within microvascular resistance networks. In skeletal muscle of the mouse, the present study demonstrates that selective disruption of the endothelium midway along arterioles effectively compromised conducted vasodilation. Furthermore, Cx37, Cx40, and (occasionally) Cx43 were expressed at the borders of arteriolar endothelial cells but not in smooth muscle cells or in capillary or venular endothelium. These findings indicate an integral role for the arteriolar endothelium in coordinating the distribution and magnitude of muscle blood flow.

Cellular Pathway(s) for Conduction

The arteriolar network is composed of resistance segments arranged in series and in parallel. When vasodilation is constrained to the vicinity of a stimulus, there is little increase in blood flow to the affected region. In contrast, the conduction of vasodilation along and between arteriolar branches promotes increases in flow through the region from which the signal originated (20). In the hamster cheek pouch, the conduction of vasodilation reflects the initiation of hyperpolarization and its transmission from cell to cell along the vessel wall (27, 33, 35). Experiments with LDT (2, 4) and intracellular recording (33) in cheek pouch arterioles have revealed that an intact endothelium is essential for initiating vasodilation with ACh but that either smooth muscle or the endothelium can provide the conduction pathway.

The present experiments are the first to investigate the cellular pathway for conduction in skeletal muscle of the mouse. Both functional studies with LDT and whole-mount immunolabeling for connexin expression indicate that the endothelium serves as the cellular pathway for conduction. Unlike the cheek pouch (an epithelial tissue), the presence of skeletal muscle fibers presents a barrier to LDT of arteriolar smooth muscle. Nevertheless, our finding that selective disruption of the endothelium interrupted conduction further supports the conclusion that the smooth muscle layer did not provide an effective alternative pathway. In feed arteries supplying the hamster retractor muscle, integrity of the endothelium is also essential for the conduction of vasodilation in response to ACh as well as ascending vasodilation in response to muscle contraction (12, 28). As indicated by labeling with propidium iodide (Fig. 2), disruption of conduction can occur well before exogenous dye can permeate endothelial cell membranes.

For vasodilation to occur in response to conduction along the endothelium, a mechanism is required for transmitting a signal for relaxation to the surrounding smooth muscle cells. As shown in other models, this heterocellular signaling can occur through myoendothelial gap junction channels (9, 11, 25) or via the release of vasodilator autacoids as the signal spreads (4). The nature of coupling between the smooth muscle and endothelium remains to be defined in arterioles in the mouse.

Immunohistochemical Localization of Connexin Isoform Expression

Each of the connexins examined here have been reported to be expressed in the endothelium of conduit and resistance arteries in a variety of mammalian species (16, 17, 25). Arterioles of the hamster cheek pouch also express all three connexin isoforms in the endothelium (25). In contrast, arterioles in the rat mesentery express Cx40, Cx43, and (occasionally) Cx37 in endothelium, but these proteins are not expressed in smooth muscle (16). Others have reported sparse immunolabeling for Cx43 and Cx40 in rat pial and cremaster arterioles (22), Cx43 labeling in endothelium of human fetal telencephalon microvessels (32), and Cx40, but not Cx37 or Cx43, labeling in mouse kidney arterioles (19). Collectively, the limited information regarding connexin expression in the microcirculation indicates that heterogeneity can exist in the pattern of isoform expression between tissues and species.

The roles of respective connexin isoforms in cardiovascular function have been investigated by genetic knockout using the mouse as a model system (7, 13, 21). Nevertheless, there is little information regarding the constitutive profile of connexin isoform expression in the mouse microcirculation. The present study is the first to characterize the constitutive expression profile of multiple connexins in the microcirculation of mouse skeletal muscle. We show that both Cx40 and Cx37 are expressed throughout arteriolar branches, whereas Cx43 expression is constrained to the larger, proximal arterioles. In the mouse cremaster muscle, a key role for Cx40 has been implicated in the conduction of vasodilation (7, 13). However, roles for Cx37 and Cx43 remain to be defined.

The restriction of Cx43 expression to proximal arterioles (Fig. 4*A*) is unlikely to affect electrical coupling but may result in regional differences in gap junctional permeability (e.g., to second messengers) and the regulation of cell-to-cell coupling by physiological stimuli (5, 15). Although the functional significance of Cx43 in the microcirculation has not yet been established, endothelial cell-specific knockout of Cx43 indicates a role for Cx43 in cardiovascular homeostasis (21). For mice in which the coding region of Cx43 was replaced with a *LacZ* reporter gene, expression was restricted largely to capillaries and small vessels in all adult organs examined; however, skeletal muscle was not examined (30). The consistency of Cx43 expression in the mesothelium lining the internal surface of the cremaster muscle (Fig. 4*B*) is consistent with previous evidence for its expression in epithelial tissues (6, 10) and implies functional coupling within this cell layer that also remains to be defined.

The apparent lack of connexin labeling in capillaries found here is notable, given the evidence that capillaries conduct vasomotor stimuli (3, 29). This inconsistency may be explained by a level of connexin expression that is below the limit of visual detection, as cells can be coupled electrically through isolated gap junction channels that are not apparent with immunolabeling (34). Indeed, the smooth muscle cell layer of hamster cheek pouch arterioles can be highly effective as a conduction pathway (2, 4, 33) despite the extremely low incidence of gap junction plaques within this layer (25).

In summary, the present study demonstrates that arterioles of the mouse cremaster muscle conduct vasodilation along the endothelial cell layer but not the smooth muscle cell layer. Conduction of vasodilation along the endothelium coincides with the expression profiles of Cx37 and Cx40 in all arteriolar branches, whereas Cx43 is expressed with variable consistency in the endothelium of the larger, proximal arteriolar branches but not in smaller, distal branches. Connexin expression was not apparent in smooth muscle cells or in capillary and venular endothelium. This pattern of connexin expression implies an integral role for the conduction of vasodilation along arteriolar endothelium in coordinating the magnitude and distribution of muscle blood flow in accord with the local demands of skeletal muscle fibers.

GRANTS

This work was supported by National Institutes of Health Grants R01-HL-41026 and R21-AG-19347. R. C. Looft-Wilson was supported by National Institutes of Health postdoctoral National Research Service Award F32-HL-67626.

REFERENCES

1. **Anderson KM and Faber JE.** Differential sensitivity of arteriolar α1- and α2-adrenoceptor constriction to metabolic inhibition during rat skeletal muscle contraction. *Circ Res* 69: 174–184, 1991.
2. **Bartlett IS and Segal SS.** Resolution of smooth muscle and endothelial pathways for conduction along hamster cheek pouch arterioles. *Am J Physiol Heart Circ Physiol* 278: H604–H612, 2000.
3. **Beach JM, McGahren ED, and Duling BR.** Capillaries and arterioles are electrically coupled in hamster cheek pouch. *Am J Physiol Heart Circ Physiol* 275: H1489–H1496, 1998.
4. **Budel S, Bartlett IS, and Segal SS.** Homocellular conduction along endothelium and smooth muscle of arterioles in hamster cheek pouch: unmasking an NO wave. *Circ Res* 93: 61–68, 2003.
5. **Burt JM, Fletcher AM, Steele TD, Wu Y, Cottrell GT, and Kurjiaka DT.** Alteration of Cx43:Cx40 expression ratio in A7r5 cells. *Am J Physiol Cell Physiol* 280: C500–C508, 2001.
6. **Cyr DG, Hermo L, and Laird DW.** Immunocytochemical localization and regulation of connexin43 in the adult rat epididymis. *Endocrinology* 137: 1474–1484, 1996.

7. **De Wit C, Roos F, Bolz SS, Kirchhoff S, Kruger O, Willecke K, and Pohl U.** Impaired conduction of vasodilation along arterioles in connexin40-deficient mice. *Circ Res* 86: 649–655, 2000.
8. **Dhein S.** Gap junction channels in the cardiovascular system: pharmacological and physiological modulation. *Trends Pharmacol Sci* 19: 229–241, 1998.
9. **Dora KA, Doyle MP, and Duling BR.** Elevation of intracellular calcium in smooth muscle causes endothelial cell generation of NO in arterioles. *Proc Natl Acad Sci USA* 94: 6529–6534, 1997.
10. **Dufresne J, Finnson KW, Gregory M, and Cyr DG.** Expression of multiple connexins in the rat epididymis indicates a complex regulation of gap junctional communication. *Am J Physiol Cell Physiol* 284: C33–C43, 2003.
11. **Emerson GG and Segal SS.** Electrical coupling between endothelial cells and smooth muscle cells in hamster feed arteries: role in vasomotor control. *Circ Res* 87: 474–479, 2000.
12. **Emerson GG and Segal SS.** Endothelial cell pathway for conduction of hyperpolarization and vasodilation along hamster feed artery. *Circ Res* 86: 94–100, 2000.
13. **Figueroa XF, Paul DL, Simon AM, Goodenough DA, Day KH, Damon DN, and Duling BR.** Central role of connexin40 in the propagation of electrically activated vasodilation in mouse cremasteric arterioles in vivo. *Circ Res* 92: 793–800, 2003.
14. **Folkow B, Sonnenschein RR, and Wright DL.** Loci of neurogenic and metabolic effects on precapillary vessels of skeletal muscle. *Acta Physiol Scand* 81: 459–471, 1971.
15. **Gu H, Ek-Vitorin JF, Taffet SM, and Delmar M.** Coexpression of connexins 40 and 43 enhances the pH sensitivity of gap junctions: a model for synergistic interactions among connexins. *Circ Res* 86: E98–E103, 2000.
16. **Gustafsson F, Mikkelsen HB, Arensbak B, Thuneberg L, Neve S, Jensen LJ, and Holstein-Rathlou NH.** Expression of connexin 37, 40, and 43 in rat mesenteric arterioles and resistance arteries. *Histochem Cell Biol* 119: 139–148, 2003.
17. **Hill CE, Rummery N, Hickey H, and Sandow SL.** Heterogeneity in the distribution of vascular gap junctions and connexins: implications for function. *Clin Exp Pharmacol Physiol* 29: 620–625, 2002.
18. **Hungerford JE, Sessa WC, and Segal SS.** Vasomotor control in arterioles of the mouse cremaster muscle. *FASEB J* 14: 197–207, 2000.
19. **Hwan Seul K and Beyer EC.** Heterogeneous localization of connexin40 in the renal vasculature. *Microvasc Res* 59: 140–148, 2000.
20. **Kurjiaka DT and Segal SS.** Conducted vasodilation elevates flow in arteriole networks of hamster striated muscle. *Am J Physiol Heart Circ Physiol* 269: H1723–H1728, 1995.
21. **Liao Y, Day KH, Damon DN, and Duling BR.** Endothelial cell-specific knockout of connexin 43 causes hypotension and bradycardia in mice. *Proc Natl Acad Sci USA* 98: 9989–9994, 2001.
22. **Little TL, Beyer EC, and Duling BR.** Connexin 43 and connexin 40 gap junctional proteins are present in arteriolar smooth muscle and endothelium in vivo. *Am J Physiol Heart Circ Physiol* 268: H729–H739, 1995.
23. **Little TL, Xia J, and Duling BR.** Dye tracers define differential endothelial and smooth muscle coupling patterns within the arteriolar wall. *Circ Res* 76: 498–504, 1995.
24. **Saez JC, Berthoud VM, Branes MC, Martinez AD, and Beyer EC.** Plasma membrane channels formed by connexins: their regulation and functions. *Physiol Rev* 83: 1359–1400, 2003.
25. **Sandow SL, Looft-Wilson R, Doran B, Grayson TH, Segal SS, and Hill CE.** Expression of homocellular and heterocellular gap junctions in hamster arterioles and feed arteries. *Cardiovasc Res* 60: 643–653, 2003.
26. **Schraufnagel DE, Roussos C, Macklem PT, and Wang NS.** The geometry of the microvascular bed of the diaphragm: comparison to intercostals and triceps. *Microvasc Res* 26: 291–306, 1983.
27. **Segal SS and Duling BR.** Flow control among microvessels coordinated by intercellular conduction. *Science* 234: 868–870, 1986.
28. **Segal SS and Jacobs TL.** Role for endothelial cell conduction in ascending vasodilatation and exercise hyperaemia in hamster skeletal muscle. *J Physiol* 536: 937–946, 2001.
29. **Song H and Tyml K.** Evidence for sensing and integration of biological signals by the capillary network. *Am J Physiol Heart Circ Physiol* 265: H1235–H1242, 1993.
30. **Theis M, de Wit C, Schlaeger TM, Eckardt D, Kruger O, Doring B, Risau W, Deutsch U, Pohl U, and Willecke K.** Endothelium-specific replacement of the connexin43 coding region by a *lacZ* reporter gene. *Genesis* 29: 1–13, 2001.
31. **Van Teeffelen JW and Segal SS.** Interaction between sympathetic nerve activation and muscle fibre contraction in resistance vessels of hamster retractor muscle. *J Physiol* 550: 563–574, 2003.
32. **Virgintino D, Robertson D, Errede M, Benagiano V, Bertossi M, Ambrosi G, and Roncali L.** Expression of the gap junction protein connexin43 in human telencephalon microvessels. *Microvasc Res* 62: 435–439, 2001.
33. **Welsh DG and Segal SS.** Endothelial and smooth muscle cell conduction in arterioles controlling blood flow. *Am J Physiol Heart Circ Physiol* 274: H178–H186, 1998.
34. **Williams EH and DeHaan RL.** Electrical coupling among heart cells in the absence of ultrastructurally defined gap junctions. *J Membr Biol* 60: 237–248, 1981.
35. **Xia J and Duling BR.** Electromechanical coupling and the conducted vasomotor response. *Am J Physiol Heart Circ Physiol* 269: H2022–H2030, 1995.
36. **Xia J, Little TL, and Duling BR.** Cellular pathways of the conducted electrical response in arterioles of hamster cheek pouch in vitro. *Am J Physiol Heart Circ Physiol* 269: H2031–H2038, 1995.